Invited paper

LARGE-EDDY-SIMULATION OF TURBULENT MAGNETOHYDRODYNAMIC FLOWS

by

Johannes WOELCK [*] ***and Gunther BRENNER***

Department of Applied Mechanics, Faculty of Mechanical Engineering,
Clausthal University of Technology, Clausthal-Zellerfeld, Germany

Original scientific paper
https://doi.org/10.2298/TSCI161215092W

A magnetohydrodynamic turbulent channel flow under the influence of a wall-normal magnetic field is investigated using the Large-Eddy-Simulation technique and k-equation subgrid-scale-model. Therefore, the new solver MHDpisoFoam is implemented in the OpenFOAM CFD-Code. The temporal decay of an initial turbulent field for different magnetic parameters is investigated. The rms values of the averaged velocity fluctuations show a similar, trend for each coordinate direction. 80% of the fluctuations are damped out in the range between $0 < Ha < 75$ *at* $Re = 6675$*. The trend can be approximated via an exponential of the form* $\exp(-a \cdot Ha)$*, where a is a scaling parameter. At higher Hartmann numbers the fluctuations decrease in an almost linear way. Therefore, the results of this study show that it may be possible to construct a general law for the turbulence damping due to action of magnetic fields.*

Key words: *magnetohydrodynamics, Hartmann flow, periodic channel flow, Large-Eddy-Simulation, k-equation subgrid-scale model, Open-FOAM, MHDpisoFoam*

Introduction

The influence of static magnetic fields on turbulent flows, which occur in numerous astrophysical, geophysical and technological applications, has received the attention of many researchers in the field of magnetohydrodynamics (MHD) since Hartmann and Lazarus [1, 2] discovered that a turbulent flow can be forced to a laminar one by the action of an applied magnetic field in 1937. The Lorentz forces arising from the induced currents in electrically conducting fluids lead to additional Joule dissipation and tend to suppress flow gradients along the direction of the magnetic field lines.

The transition behavior is, for example, a relevant problem in the field of metallurgy for flow control and crystal growth, as well as for liquid metal flows in fusion reactor blankets. It is also of interest in the general context of shear flow transition, because the magnetic field may modify the mechanisms that have been identified as important in subcritical transition of non-conducting shear flows.

*Corresponding author, e-mail: johannes.woelck@tu-clausthal.de
Both authors equally contributed to this paper.

Recent numerical studies have been performed, focusing on the transition in MHD periodic channel flows with a uniform, wall-normal magnetic field. This so-called Hartmann flow is considered as a prototypical MHD shear flow. When the magnetic field is sufficiently strong, it modifies in the laminar case the Poiseuille velocity profile and gives a rise to the boundary layers, where Lorentz and viscous forces balance. The thickness of these layers is inversely proportional to the magnetic induction. Turbulent fluctuations become strongly anisotropic or even quasi-2D under the action of applied magnetic fields.

This study investigates the transition phenomenon in the case of low magnetic Reynolds numbers using Large-Eddy-Simulations (LES). In contrast to the related work in the field of MHD, the induction equation is used instead of the electric potential equation. This brings the advantage of directly relating the main hydrodynamic quantity to the magnetic one. Furthermore, the clear analogy between the induction and the Navier-Stokes equation allows an easy implementation in an existing CFD-Code, here in the pisoFoam solver of OpenFOAM-4.1, and adapting the same discretization and segregated solution techniques as in the hydrodynamic case.

For weak magnetic fields it is shown by experiments [3-5] and a few direct numerical studies [6-11], that MHD turbulence does not differ from non-magnetic turbulence. Therefore, there is no need to modify existing LES models to take MHD effects into account. The influence of LES subgrid-scale (SGS) models on the flow prediction have been investigated by few researchers. Shimomura [12] and Kobayashi [13] already tested the classical Smagorinsky model (SM) for a periodic Hartmann flow. Both concluded that this model is not adequate to predict turbulent MHD flows, mainly because the value of the Smagorinsky constant remains unchanged over the simulation time and is not adapted to MHD turbulence damping effects. On the contrary, the dynamic Smagorinsky model (DSM) used by Knaepen and Moin [14], Kobayashi [13] as well as Sarris *et al*. [15] is reported to work well since the Smagorinsky constant automatically decreases while the magnetic field increases. Therefore, the DSM might be able to automatically switch off when the turbulent flow is forced to a laminar one by the action of the magnetic field. Thus, the DSM shows the potential to reproduce the transition from turbulent MHD flow to a laminarized one without special treatment for the magnetic field.

The DSM is not implemented in the OpenFOAM-code. Therefore, a different OpenFOAM SGS model is used here, namely the dynamic k-equation SGS model. Due to the extra resolved transport equation in the dynamic k-equation SGS model, a more accurate time scale to the unresolved scales compared to the dynamic SM is expected. To prove this assumption, experimental results or direct numerical simulations are necessary, which should be performed in future works.

This work focuses on the case of homogeneous, initially isotropic, decaying turbulence and the flow in a periodic channel. The evolution of the turbulent velocity fluctuations is investigated for increasing magnetic field values.

This work is organized as follows. First, the governing equations for MHD flows are derived and the LES approach as well as SGS model for MHD turbulence are summarized. In the section *Implementation* the discretization and the solution procedure for the MHD equations as well as their implementation in OpenFOAM is described. Furthermore, using the analytical Hartmann solution for laminar MHD flows, the implementation is verified in the section *Verification*. The numerical results for the periodic channel are presented and discussed in the section *Numerical results*. Finally, the paper is ended with conclusions and further remarks.

Mathematical and numerical background

Magnetohydrodynamics

This paper considers the Newtonian flow of an electrically conduction fluid and assumes that the applied magnetic field is uniform and orthogonal to the flow direction. Furthermore, it is assumed that the applied magnetic field is uniform and orthogonal to the flow direction. Considering the low magnetic Reynolds number $R_m = \mu_m \sigma_e L_0 u_0$ case, the governing equations can be simplified using the in ductless approximation. The magnetic Reynolds number is a dimensionless scaling parameter representing the relative strength of advection and diffusion in the induction equation. The σ_e is hereby the electric conductivity and u_0 and L_0 the characteristic velocity and length scale, respectively.

Perturbations of the magnetic field induced by the fluids motion are small in comparison with the imposed magnetic field and can therefore be neglected [16]. Then, the flow is governed by the Navier-Stokes (1) and continuity equation (2), representing the momentum and mass conservation:

$$\frac{\partial \mathbf{u}}{\partial t} + (\mathbf{u}\cdot\nabla)\mathbf{u} - \nu\nabla^2\mathbf{u} - \frac{1}{\rho}\mathbf{f}_L = -\frac{1}{\rho}\nabla p \tag{1}$$

$$\nabla\cdot\mathbf{u} = 0 \tag{2}$$

$$\mathbf{f}_L = \mathbf{j}\times\mathbf{B} \tag{3}$$

Here p, ρ, and ν denote the pressure, density, and kinematic viscosity. The fields of velocity, electric current density, and magnetic induction are represented by **u**, **j**, and **B**. Coupling between the velocity and magnetic field is realized by the Lorentz force, eq. (3), which acts perpendicular to the magnetic field lines.

Under the present conditions of a small magnetic Reynolds number $R_m \ll 1$ the electric current density can be expressed by Ampere's law (4) under the in ductless MHD assumptions according to [16, 17], which is one of the classical Maxwell equations:

$$\nabla\times\mathbf{B} = \mu_m\mathbf{j} \tag{4}$$

Replacing the current density in eq. (1) and after some analytical manipulation, the Lorentz force $\mathbf{f}_L$ can be expressed as:

$$\mathbf{f}_L = \mathbf{j}\times\mathbf{B} = -\frac{1}{\mu_m}\mathbf{B}\times\nabla\times\mathbf{B} = -\nabla\left(\frac{1}{2\mu_m}B^2\right) + \frac{1}{\mu_m}\nabla\cdot(\mathbf{BB}) \tag{5}$$

Note that (**BB**) is the dyadic product of the vector **B** with itself. Analyzing eq. (5) the first term on the right side can be identified as being the gradient of a scalar and the last term as a stress tensor. In literature, these two terms are called the magnetic pressure and the Maxwell stress tensor, respectively [18].

To obtain the evolution of the magnetic field it is necessary to solve an additional transport equation, which is called the induction, eq. (6), and can be deduced from the Maxwell equations. Namely the laws of Ohm $\mathbf{j} = \sigma_e(\mathbf{E} + \mathbf{u}\times\mathbf{B})$, Ampere $\nabla\times\mathbf{B} = \mu_m\mathbf{j}$, and Faraday $\nabla\times\mathbf{E} = \partial\mathbf{B}/\partial t$:

$$\frac{\partial \mathbf{B}}{\partial t} - \nabla \times (\mathbf{u} \times \mathbf{B}) + \Gamma_m \nabla \times (\nabla \times \mathbf{B}) = 0 \tag{6}$$

In analogy to other diffusive processes, like heat conduction, the quantity $\Gamma_m = (\mu_m \sigma_e)^{-1}$ in eq. (6) can be interpreted as a kind of magnetic diffusivity.

For a precise description of MHD phenomena, the Gauss law for magnetic fields, eq. (7), must be satisfied, which is also one of the Maxwell equations and describes the solenoidal nature of the magnetic field. Even small deviations from this condition can produce large errors in the solution of the MHD equations, resulting in unphysical forces parallel to the magnetic field [19].

Using the vector identities:

$$\nabla \times \nabla \times \mathbf{B} = -\nabla^2 \mathbf{B} \tag{8}$$

$$\nabla \times (\mathbf{u} \times \mathbf{B}) = (\mathbf{B} \cdot \nabla)\mathbf{u} - (\mathbf{u} \cdot \nabla)\mathbf{B} \tag{9}$$

and eq. (2) as well as eq. (7) the Helmholtz formulation (10) of the induction equation can be obtained, which looks similar to the Navier-Stokes equation [20]:

$$\frac{\partial \mathbf{B}}{\partial t} - (\mathbf{u} \cdot \nabla)\mathbf{B} - \Gamma_m \nabla^2 \mathbf{B} - (\mathbf{B} \cdot \nabla)\mathbf{u} = 0 \tag{10}$$

The induction equation in Helmholtz form (10) describes the temporal evolution of the magnetic field $\partial \mathbf{B}/\partial t$ due to advection $(\mathbf{u}\cdot\nabla)\mathbf{B}$ and diffusion $\Gamma_m \nabla^2 \mathbf{B}$. The last term on the right side of eq. (10) represents sources $(\mathbf{B}\cdot\nabla)\mathbf{u}$, which are generated by mechanical stretching of the magnetic field lines due to the velocity field.

In contrast to the above shown formulation of the MHD equations used in almost all studies concerning MHD turbulence, an alternative formulation is used in the following, where the electric field is represented by the potential φ. This leads to a Poison equation (11) defining the electric potential φ and to a modified form of Ohm's law (12):

$$\nabla^2 \varphi = \nabla \cdot (\mathbf{u} \times \mathbf{B}) \tag{11}$$

$$\mathbf{j} = -\nabla \varphi + \mathbf{u} \times \mathbf{B} \tag{12}$$

If the magnetic field is static, this formulation explicitly guarantees $\nabla \cdot \mathbf{B} = 0$, but requires additional boundary conditions for φ. These need special, complicated treatment to ensure that the induced magnetic field vanishes at the boundaries. Therefore, in this study the induction equation is chosen for defining the main electromagnetic quantity **B**. This brings the advantage of directly relating the main hydrodynamic quantity **u** to the magnetic one **B**. Furthermore, the analogy between induction (10) and Navier-Stokes (1) equations allows an easy implementation in an existing CFD-Code, here in the pisoFoam solver of OpenFOAM-4.1, and adapting the segregated approach for an effective solution.

Large-Eddy-Simulation

The main idea of Large Eddy Simulations (LES) is to compute or resolve the large--grid-scale (GS) features of the flow directly, whereas the dissipation scales are substituted by

specific sub-grid-scale (SGS) models. Via low-pass filtering of the Navier-Stokes equation (1) GS $\bar{\mathbf{f}}$ and SGS $\mathbf{f}'$ features can be separated, *i. e.* $\mathbf{f} = \bar{\mathbf{f}} + \mathbf{f}'$ This is done by evaluating the convolution integral:

$$\overline{\mathbf{f}(\mathbf{x})} = \oint G(\mathbf{x}, \mathbf{x}'; \nabla) f(x) \mathrm{d}x \Leftrightarrow \oint G(x, x; \nabla) \mathrm{d}x = 1 \tag{13}$$

over the whole computational domain. Here, Δ is the filter width and $G = G(\mathbf{x}, \Delta)$ is the filter kernel.

As discussed in the section *Introduction* there is no need to modify the existing LES models to take MHD effects into account. Therefore, the LES form of the Navier-Stokes equation with added Lorentz force, eq. (1), for the resolved velocity field $\bar{\mathbf{u}}$ is obtained after a spatial filter operation by:

$$\frac{\partial \bar{\mathbf{u}}}{\partial t} + (\bar{\mathbf{u}} \cdot \nabla)\bar{\mathbf{u}} - \nu \nabla^2 \bar{\mathbf{u}} + \nabla \cdot \boldsymbol{\tau} - \frac{1}{\rho} \bar{\mathbf{f}}_L = -\frac{1}{\rho} \nabla \bar{p} \tag{14}$$

Note, that $\overline{\mathbf{u}\mathbf{u}} \neq \bar{\mathbf{u}}\,\bar{\mathbf{u}}$ and cannot be determined numerically. Therefore, a modeling approximation must be used for this term. The difference between both sides of the inequality leads to the SGS stress tensor:

$$\boldsymbol{\tau} = \overline{\mathbf{u}\mathbf{u}} - \bar{\mathbf{u}}\,\bar{\mathbf{u}} \tag{15}$$

To close eq. (14) the SGS stress tensor must be expressed in terms of the resolved velocity $\bar{\mathbf{u}}$ to remove the energy from the resolved scales, mimicking the drain associated with Kolmogorov cascade. A variety of so-called SGS models have been proposes in the literature for this purpose.

To improve the accuracy of the Smagorinsky model, one equation models were developed. Most of them are based on the eddy-viscosity concept and drop the assumption of equilibrium regarding the unresolved scales. To prove the accuracy, an extra transport equation for subgrid turbulence is added. One of the quantities often chosen is the subgrid-scale kinetic energy, which is defined as:

$$k = 0.5 \mathrm{tr}(\boldsymbol{\tau}) \tag{16}$$

The eddy-viscosity can then be transformed into the form:

$$\nu_\tau = C_k \Delta \sqrt{k} \tag{17}$$

According to Horiuti [21] the k-transport equation is defined by eq. (18):

$$\frac{\partial k}{\partial t} + (\bar{\mathbf{u}} \cdot \nabla)k = 0.5 \mathrm{tr}(\boldsymbol{\tau}\bar{\mathbf{S}}) + \left[(C_{kk} \Delta \sqrt{k} + \nu) \right] \nabla^2 k - C_\epsilon \frac{k^{3/2}}{\Delta} \tag{18}$$

The values of the different constants are typically $C_K = 0.05$, $C_\varepsilon = 1.0$, and $C_{kk} = 0.1$, respectively. Although this model suffers from the same deficiencies as the Smagorinsky model, it provides a more accurate time scale to the unresolved scale-model through the independents definition of the velocity scale in the extra transport equation. A study by Fureby [22] has shown the one-equation model to be effective and superior to the SM model.

In the dynamic form of this model the coefficient C_K is dynamically recalculated as part of the flow calculations. In this study the dynamic procedure proposed by Germano *et al*.

[23] and the least-square technique suggested by Lilly [24] is used to compute the dynamic constant C_K:

$$C_K = \frac{\langle \mathbf{LM} \rangle}{\langle \mathbf{MM} \rangle} \tag{19}$$

where **L** and **M** are given by:

$$\mathbf{L} = \widehat{\mathbf{uu}} - \hat{\mathbf{u}}\hat{\mathbf{u}}\mathbf{M} = 2\hat{\bar{\Delta}}^2 \left|\hat{\bar{\mathbf{S}}}\right| \hat{\bar{\mathbf{S}}} \tag{20}$$

Here, the test-filtered $\hat{\mathbf{u}}$ are calculated using a box filter in physical space. The test-filter width is twice the size of the grid size.

Implementation

Equations (1) and (10) along with the continuity constraints for the magnetic, eq. (7), and velocity field, eq. (2), are representing the governing system of the MHD equations. To describe the MHD effects properly, inter-equation coupling between the equations is necessary. In the present work, therefore, the pisoFoam solver of the OpenFOAM-4.1 release is modified and merged with the mhdFoam solver to MHDpisoFoam. This solver can treat different incompressible flow problems and includes a variety of turbulence models. The hydrodynamic equations are discretized using the finite-volume method (FVM) and solved in a segregated approach using the pressure implicit with splitting operators (PISO) algorithms according to Issa [25]. Due to the obvious analogy between the Navier-Stokes eq. (1) and induction equation (10) it is possible to use the same discretization technique and solution algorithms for the magnetic part, which is described in detail for example in [26-28]. Therefore, another loop (BPISO) is added to the solution algorithm to solve the induction equation.

Both equations are discretized and represented in OpenFOAM-Syntax according to listing 1 and 2, respectively. Note, that phi is the volume velocity flux defined on the faces of each cell and is a result of the discretization procedure, since in FVM the Gauss theorem is used to transform volume into surface integrals. Likewise, phiB defines the magnetic flux through the cell faces. In order to obtain an efficient solution and to avoid staggering on collocated meshes, a Rhie and Chow [29] approach is used to interpolate the face values of the magnetic field. Therefore, the pressure gradient ∇p is not present in listing 1. An additional pressure equation is constructed and solved in the segregated approach. Afterwards, the velocity field is corrected with this solution. This requires the solution of a pressure equation for **B**, such that a new and fictitious pseudo-magnetic pressure p_B is introduced to derive a flux equation from the solenoidal constraint. Both the induction and pseudo-magnetic pressure equation are coupled together in the BPISO loop. Therefore, the fluxes exactly obey the free-divergen-

```
fvVectorMatrixUEqn
(
fvm::ddt(U) + fvm::div(phi, U)
+ turbulence−>divDevReff(U)
− fvc::div(phiB,2.0*DBU*B)
+ fvc::grad(DBU*magSqr(B))
);
```

Listing 1: Navier-Stokes equation (1)

```
fvVectorMatrixBEqn
(
fvm::ddt(B)
      + fvm::div(phi,B)
      − fvc::div(phiB,U)
      − fvm::laplacian(DB,B)
);
```

Listing 2: Induction equation (10)

ce constraint of the magnetic field $\nabla \cdot \mathbf{B} = 0$, whereas the p_B field is non-zero and represents the discretization error as the difference between fluxes and interpolated cell-centered values. However, it approaches zero when the system of equations is iterated to convergence. Note, that no additional correction of **B** is necessary, since p_B has impact on this field and is only introduced to get the fluxes phiB.

Due to the nature of the magnetic field, fluxes at the boundaries should be orthogonal to the magnetic field lines. Therefore, at these boundaries the Neumann condition $\nabla p_B = 0$ must be applied and all others the Dirichlet condition $p_B = 0$.

Furthermore, all spatial derivatives are discretized in OpenFOAM using the implemented second-order differencing scheme. Whereas the time is advanced by a second-order Adam-Bashworth scheme.

Verification

To verify the implemented model, the laminar Hartmann case is considered. This is a flow between two walls which is modified by a magnetic field perpendicular to the streamwise direction of the flow. The analytical solution for the velocity profile for the fully-developed flow is, according to Hartmann [2] defined by:

$$\frac{u}{u_0} = \frac{\mathrm{Ha}[\cosh(\mathrm{Ha}) - \cosh(\mathrm{Ha} \cdot y/L)]}{\mathrm{Ha}\cosh(\mathrm{Ha}) - \sinh(\mathrm{Ha})} \tag{21}$$

where L is the characteristic length scale and u_0 the velocity scale.

Expression $\mathrm{Ha} = LB_0[\sigma_e/(\rho\nu)]^{1/2}$ represents the Hartmann number, which is a measure for the ratio between viscous and electromagnetic forces. As shown in fig. 1 perfect agreement between analytical and numerical results is observed. Furthermore, this example shows how in a bounded laminar flow with a prescribed flow rate the magnetic field changes the slope of the velocity profile from Poiseuille to a plug flow.

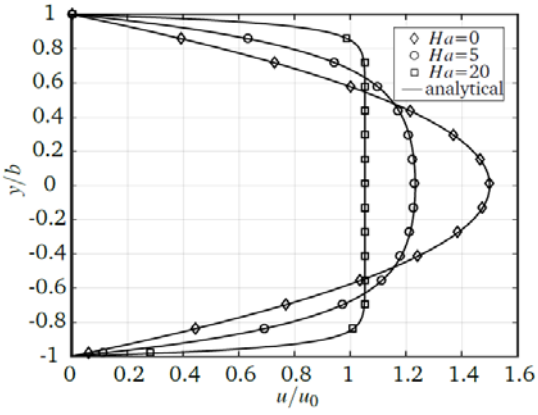

Figure 1. Velocity profiles for various Ha

Numerical results

To demonstrate the ability of the implemented OpenFOAM solver MHDpisoFoam together with the dynamic k-equation SGS model to perform MHD LES, an incompressible channel flow is investigated. A case comparable to the DNS by Dong *et al*. [11] and Kenjeres *et al*. [30] as well to the LES by Knaepen *et al*. [14], Kobayashi [13], and Krasnov [31] is constructed. The configuration is shown in fig. 2, where x, y, and z denote the streamwise, spanwise, and wall-normal directions, respectively. Periodic boundary conditions are imposed in x- and z-directions. The artificially created inflow boundary condition mimics the assumed flow between the infinitely extend horizontal walls only if the computational domain is large enough to obtain a turbulent state without long-range spatial correlations. This is why

$2L\pi \times L\pi \times L$ is chosen for computational domain dimensions in compliance with Krasnov *et al*. [31], with a channel width of $L = 2$ m.

In x- and z-direction $N_x = 40$ and $N_z = 30$ cells are distributed uniformly, whereas $N_y = 50$ cells with non-uniform spacing are placed in y-direction, which agglomerate near the wall. A comparison of the results generated via DNS and LES by Krasnov *et al*. [32] with the results discussed later in this section show that the here chosen grid resolution is not adequate to capture the Hartmann shear layers. The thickness of these layers is defined by:

$$\delta = \frac{1}{B_0}\sqrt{\frac{\rho\nu}{\sigma_e}} \tag{22}$$

and requires at least nine computational cells for a proper resolution. Since this study focuses on MHD turbulence damping effects far away from the walls using integral values for the turbulent fluctuations, this near-wall refinement is not strictly required.

The flow in the computational domain is driven by a constant pressure gradient between the in- and outlet of the computational domain. At the walls the no-slip boundary condition $\mathbf{u} = 0$ for the velocity is applied. Furthermore, the zero gradient conditions for the hydrodynamic $\nabla p = 0$ and pseudo-magnetic pressure $\nabla p_B = 0$ are used. A uniform magnetic field of magnitude B_0 is applied in wall-normal direction. The material parameters used in this study are listed in tab. 1.

To generate a suitable, homogeneous turbulence field as initial condition, an initial simulation is executed. Starting with a random, isotropic velocity field and without an applied magnetic field this simulation is performed until a statistically steady state is reached, which can be identified by an approximate time independence of the averaged GS components of the velocity field. This data is used to initialize a set of MHD simulations at a fixed Reynolds number of Re = 6675 with increasing Hartman numbers. Averaging of the flow quantities starts only, when the transition to a new statistically stationary state is completed. For this purpose, the transient global quantities such as the kinetic energy and the mean velocity of the flow are monitored during run time. The flow statistics are collected and averaged over ten eddy turnover times $T = L/u_0$.

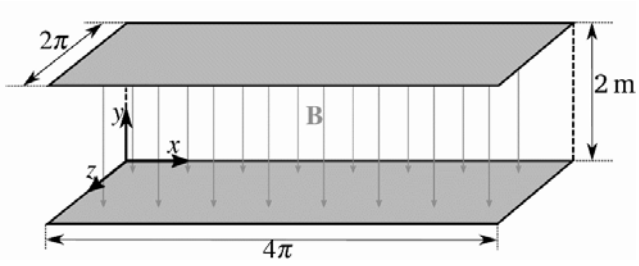

Figure 2. Periodic channel configuration

Table 1. Physical properties

Viscosity (ν)	Density (ρ)	Conductivity (σ_e)	Permeability (μ_m)
$2\cdot10^{-5}$ m^2/s	10^3 kg/m^3	10^6 A^{2}s^3/(kgm^3)	10^{-6} kgm/(A^{2}s^2)

Effect on turbulent flow structures

The effect of magnetic fields on turbulent flow structures is exemplarily shown in fig. 3 for the velocity field in the yz-plane. Two unique impacts are clearly visible. First, it is recognizable that the turbulent fluctuations in the shear layer are sufficiently reduced in

streamwise direction by increasing the magnetic field. Furthermore, the thickness of these layers is reduced. Second, these structures elongate in the direction of the magnetic field lines. The general trend is that they become larger, slower and less intense as the value of the magnetic field increases. Note, that these structures are also present in the upper right snapshot, but hardly recognizable. Further, the effect of the magnetic field seems to be stronger in the core of the channel, where the turbulence structures are suppressed to a larger degree than near the walls. These observations are in qualitative agreement to those presented by Lee and Choi [10] as well by Krasnov *et al*. [32].

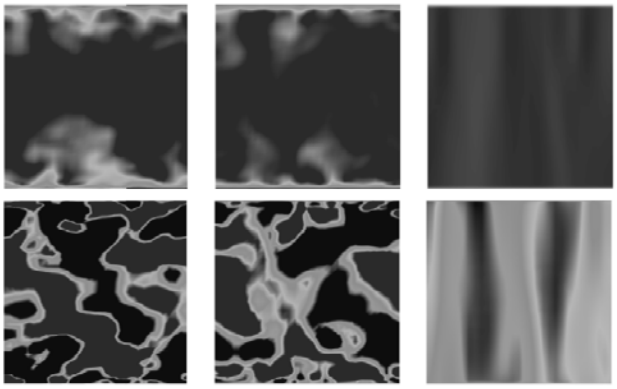

Figure 3. Development of the velocity components in the yz-plane in the middle of the channel. The upper snapshots show the streamwise component and the lower ones the wall-normal component. From left to right the Hartmann number is increasing (Ha = 0; 25; 75)

Integral characteristics

Figure 4 shows the time evolution of the mean velocity for the three coordinate directions. The data is sampled and averaged at the point (2, 1, 1) in the middle of the computational domain. Analyzing the three graphs it is obvious, that the damping effects of the magnetic field mainly takes place in the streamwise direction. As the magnetic field strength increases, the mean velocity of the streamwise component is approaching $\overline{u}_x = 0.135$ m/s. This is the specified inlet velocity, *i. e*. the specified velocity without the downstream generated fluctuations. Therefore, almost all turbulent fluctuations are significantly damped out in the streamwise direction due to the action of the magnetic field. The damping effect of the magnetic field seems to be less intense in the other two directions, as the viscosity dampens the fluctuations to zero even when no magnetic field is active.

Furthermore, fig. 4 shows that after $t = 100$ s an almost statistically, stationary state is reached. The turbulent fluctuations are filtered from the velocity field and averaged overfive eddy turnover times $T = L/u_0 = 14$ s. Figure 5 shows the root-mean-square (rms) value of the averaged velocity fluctuations u' standardized with the fluctuations u_0', which are present in the non-magnetic case. Note, that in this case the velocity field of the whole domain is used for the calculation instead of the local sampling point used before.

Generally, the same trend of the fluctuation components is conspicuous. In the range of $0 < \mathrm{Ha} < 75$, 80% of the fluctuations are damped out by the magnetic field and an almost laminar state is observable. The trend could be approximated by an exponential function of the form $f(\mathrm{Ha}) = exp(-a \cdot \mathrm{Ha})$, where $a = -0.015$ is a scaling parameter.

At higher Hartmann numbers the fluctuations decrease linearly. Therefore, it is possible to derive a general law for the magnetic damping of fluctuations. This is a first attempt and should be proven by more numerical simulations for various Hartmann and Reynolds numbers. The point of transition from the exponential to the linear course should be examined more precisely.

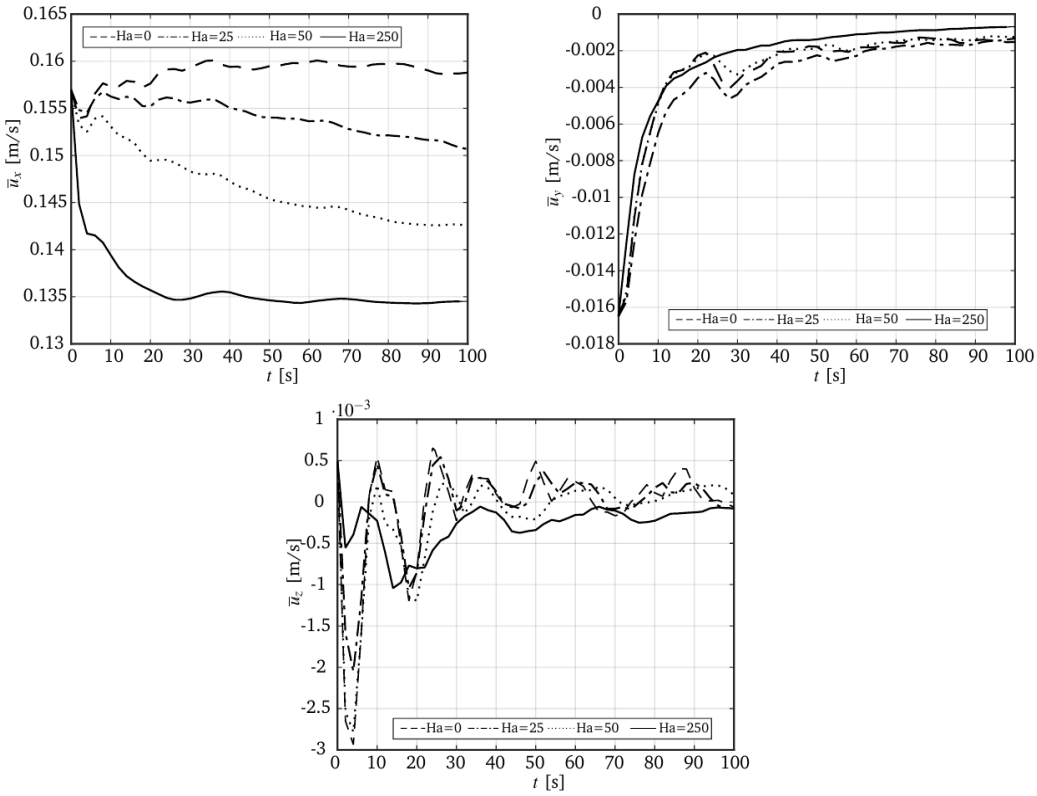

Figure 4. Temporal evolution of the mean velocity components

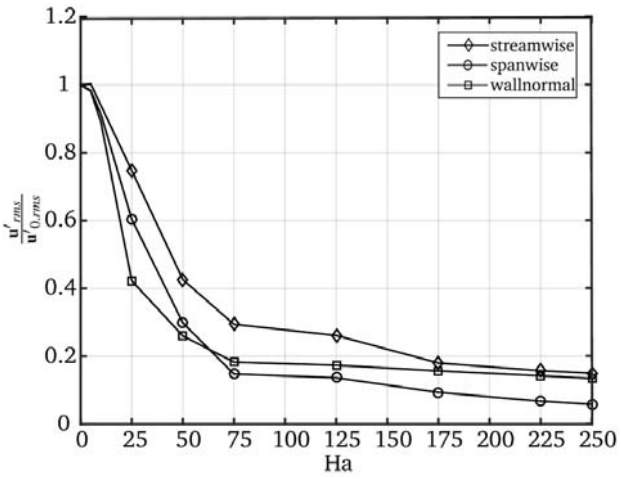

Figure 5. Evolution of the rms value of velocity fluctuations standardized with non-magnetic ones

Conclusions

A magnetohydrodynamic turbulent channel flow under the influence of a wall--normal magnetic field was investigated using the Large-Eddy-Simulation technique. There-

fore, a new solver MHDpisoFoam was implemented in the OpenFOAM CFD-code and verified against the analytic solution for the laminar flow. Using the dynamic k-equation subgrid--scale model as closure, the turbulence damping effect of the uniform magnetic fields was investigated for a generic channel flow at Re = 6675. Cyclic boundary conditions are imposed in stream- and spanwise directions to generate a self-sustaining turbulence. The initial data precursor simulation without a magnetic field was performed until a statistically steady-state was reached. This data was used as a starting condition for simulations with increasing magnetic field strengths. Temporal evolution of the mean value indicated a significant damping effect in streamwise flow direction while no significant damping effect could be observed in the other two directions. On the other hand, the rms values of the averaged velocity fluctuations have shown a similar, significant trend for each coordinate direction. Eighty percents of the fluctuations are damped out in the range between $0 < \mathrm{Ha} < 75$. The trend could be approximated via an exponential equation of the form $exp(-a \cdot \mathrm{Ha})$, where a is a scaling parameter. At higher Hartmann numbers the fluctuations decrease in an almost linear way. Therefore, the results of this study show that it may be possible to construct a general law for the magnetic turbulence damping. However, more numerical simulations are needed to derive a general law. The damping trend should be investigated for a wide range of Reynolds and Hartmann numbers.

Nomenclature

- a – scaling parameter, [–]
- $\mathbf{B}$ – magnetic field, [kg $A^{-1}s^{-2}$]
- $\mathbf{E}$ – electric field [V m^{-1}]
- $\mathbf{f}_L$ – Lorentz force, [N]
- Ha – Hartmann number, [–]
- $\mathbf{j}$ – current density, [A m^2]
- k – turbulence kinetic energy, [m^2s^{-2}]
- L – characteristic length scale, [m]
- p – pressure, [Pa]
- p_B – fictitious magnetic pressure [kg m $s^{-3}A^{-1}$]
- Re – Reynolds number, [–]
- R_m – magnetic Reynolds number, [–]
- T – eddy turnover time, [s]
- t – time, [s]
- u_0 – characteristic velocity scale, [m s^{-1}]
- $\mathbf{u}$ – velocity field, [m s^{-1}]

Greek symbols

- Γ_m – magnetic diffusivity, [m^2s^{-1}]
- δ – thickness of Hartmann layers, [m]
- μ_m – magnetic permeability, [kg m $A^{-2}s^{-2}$]
- ν – kinematic viscosity, [m^2s^{-1}]
- ν_τ – turbulent eddy-viscosity, [m^2s^{-1}]
- ρ – density, [kg m^{-3}]
- σ_e – intermittency, [A $V^{-1}m^{-1}$]
- τ – SGS stress tensor, [m s^{-1}]
- φ – electric potential, [V]

References

[1] Hartmann, J., Lazarus F., *Hg-Dynamics II Experimental Investigations on the Flow of Mercury in a Homogeneous Magnetic Field*, Levin & Munksgaard, Copenhagen, Denmark, 1937
[2] Hartmann, J., *Hg-Dynamics I. Theory of the Laminar Flow of an Electrically Conductive Liquid in a Homogeneous Magnetic Field*, Levin & Munksgaard, Copenhagen, Denmark, 1937
[3] Moloko, S., Reed, C. B., Review of Free-Surface MHD Experiments and Modeling, Technical report, Argonne National Laboratory, Argonne, Ill., USA, 2000
[4] Fautrelle, *et al.*, Free-Surface Horizontal Waves Generated by Low-frequency Alternating Magnetic Fields, *J. Fluid Mech.*, *527* (1999), Mar., pp. 285-301
[5] Andreev, O., *et al.*, Experimental Study of Liquid Metal Channel Flow under the Influence of a Nonuniform Magnetic Field, *Physics of Fluids*, *18* (2006), 6, pp. 065108-1-065108-11
[6] Vorobev, A., *et al.*, Anisotropy of Magnetohydrodynamic Turbulence at Low Magnetic Reynolds Number, *Phys. Fluids*, *17* (2005), 12, pp. 125105-1-125105-12
[7] Satake, S. I., *et al.*, Advances in Direct Numerical Simulation for MHD Modeling of Free Surface Flows, *Fusion Engineering and Design*, 61-62 (2002), Nov., pp. 95-102

[8] Krasnov, D., *et al.*, Comparative Study of Finite Difference Approaches in Simulation of Magnetohydrodynamic Turbulence at Low Magnetic Reynolds Number, *Computers & Fluids*, *50* (2011), 1, pp. 46-59
[9] Krasnov, D. S., *et al.*, Numerical Study of the Instability of the Hartmann Layer, *J. Fluid Mech.*, *504* (1999), Apr., pp. 183-211
[10] Lee, D., Choi, H., Magnetohydrodynamic Turbulent Flow in a Channel at low Magnetic Reynolds Number, *J. Fluid Mech*., *439* (2001), July, pp. 367-394
[11] Dong, S., *et al.*, Secondary Energy Growth and Turbulence Suppression in Conducting Channel Flow with Streamwise Magnetic Field, *Phys. Fluids*, *24* (2012), 7, pp. 074101-1-074101-19
[12] Shimomura, Y., Large Eddy Simulation of Magnetohydrodynamic Turbulent Channel Flows under a Uniform Magnetic Field, *Phys. Fluids A*, *3* (1991), 12, pp. 3098-3106
[13] Kobayashi, H., Large Eddy Simulation of Magnetohydrodynamic Turbulent Channel Flows with Local Subgrid-Scale Model Based on Coherent Structures, *Phys. Fluids*, *18* (2006), 4, pp. 045107-1-045107-10
[14] Knaepen, B., Moin, P., Large-Eddy Simulation of Conductive Flows at Low Magnetic Reynolds Number, *Phys. Fluids*, *16* (2004), 5, pp. 1255-1261
[15] Sarris, I. E., *et al.*, Large-eddy Simulations of the Turbulent Hartmann Flow Close to the Transitional Regime, *Phys. Fluids*, *19* (2007), 8, pp. 085109-1-085109-9
[16] Shercliff, J. A., *A Textbook of Magnetohydrodynamics*, Pergamon Press, Oxford, UK, 1965
[17] Davidson, P. A., *An Introduction to Magnetohydrodynamics*, Cambridge University Press, Cambridge, UK, 2001
[18] Muller, U., Buhler, L., *Magnetofluiddynamics in Channels and Containers*, Springer, Berlin, 2001
[19] Brackbill, J., Barnes, D., The Effect of Nonzero div·B on the Numerical Solution of the Magnetohydrodynamic Equations, *Journal of Computational Physics*, *35* (1980), 3, pp. 426-430
[20] Ben Salah, N., *et al.*, A Finite Element Method for Magnetohydrodynamics, *Computer Methods in Applied Mechanics and Engineering*, *190* (2001), 43-44, pp. 5867-5892
[21] Horiuti, K., Large Eddy Simulation of Turbulent Channel Flow by One-Equation Modeling, *J. Phys. Soc. Jpn.*, 54 (1985), 8, pp. 2855-2865
[22] Fureby, C., *Large Eddy Simulation of Magnetohydrodynamics*, FOA, Stockholm, 2000
[23] Germano, M., *et al.*, A Dynamic Subgrid-Scale Eddy Viscosity Model, *Phys. Fluids A*, *3* (1991), 7, pp. 1760-1765
[24] Lilly, D. K., A Proposed Modification of the Germano Subgrid-Scale Closure Method, *Phys. Fluids A*, *4* (1992), 3, pp. 633-635
[25] Issa, R. I., Solution of the Implicitly Discretised Fluid Flow Equations by Operator-Splitting, *Journal of Computational Physics*, *62* (1986), 1, pp. 40-65
[26] Jasak, H., Error Analysis and Estimation for the Finite Volume Method with Applications to Fluid Flows, Ph. D. thesis, Imperial College, London, 1996
[27] Ferziger, J. H., Perić, M., *Computational Methods for Fluid Dynamics*, Springer, Berlin, 1997
[28] Versteeg, H. K., Malalasekera, W., *An Introduction to Computational Fluid Dynamics: The Finite Volume Method*, Pearson/Prentice Hall, UK, 2005
[29] Rhie, C. M., Chow, W. L., Numerical Study of the Turbulent Flow Past an Airfoil with Trailing Edge Separation, *AIAA Journal*, *21* (1983), 11, pp. 1525-1532
[30] Kenjeres, S., *et al.*, A Direct-Numerical-Simulation-Based Second-Moment Closure for Turbulent Magnetohydrodynamic Flows, *Phys. Fluids*, *16* (2004), 5, pp. 1229-1241
[31] Krasnov, D., *et al.*, Magnetohydrodynamic Turbulence in a Channel with Spanwise Magnetic Field, *Phys. Fluids*, *20* (2008), 9, pp. 095105-1-095105-19
[32] Krasnov, D., *et al.*, MHD Turbulence in a Channel with Spanwise Field, WILEY-VCH Verlag, 2008

Paper submitted: December 15, 2016
Paper revised: February 17, 2017
Paper accepted: February 20, 2017